Keyang Lu[a,*], Robert H. White[b], Feng Fu[a], Junfeng Hou, Yisheng Zhang, Neil Gribbins and Zhiyong Cai*

Reinforced hybrid wood-aluminum composites with excellent fire performance

Abstract: The fire performance of several types of wood-aluminum composites (WAC) was analyzed by the small vertical furnace test. The time needed to reach the temperature of 139°C/181°C ($T_{139°C/181°C}$) and the linear char rate of 300°C ($L_{300°C}$) were obtained by evaluating the fire performance of WAC. The $T_{139°C/181°C}$ values ranged from 23.6 to 44.8 min. The presence and position of the aluminum alloy sheet remarkably affected the fire performance of WAC. In addition to an initial delay of 19 min, the $L_{300°C}$ also increased when the aluminum alloy sheet was located on the surface. However, the times for 300°C only increased slightly when the aluminum alloy sheet was in the middle. The initial delay observed for the aluminum alloy sheet on the surface was reduced by more than 50% when the wood veneer was located on the surface of the aluminum alloy sheet. The mechanical properties of WAC were also investigated. It was concluded that the uniformity and strength of different composites was improved after the lamination of the aluminum alloy sheet. In addition, the modulus of elasticity of WAC quadrupled, and the bonding strength between the aluminum alloy sheet and the oriented strand board (OSB) was greater than that of the OSB.

Keywords: aluminum alloy sheet, fire performance, mechanical property, wood-aluminum composite (WAC)

DOI 10.1515/hf-2014-0099
Received March 30, 2014; accepted November 4, 2014; previously published online December 6, 2014

Introduction

Wood-based composites possess an inherent flammability and often contribute to the propagation of fires. Thus, the fire performance of such composites plays an increasingly significant role in their engineered structural applications. Fire retardants and other nonflammable materials (i.e., concrete and metals) (Winandy et al. 2008; Urso et al. 2009; Zhang et al. 2012) may also improve their fire performance in coating, laminating, or filling. To this purpose, a mixture of calcite and various fire retardants were applied in the coating of medium-density fiberboard (MDF) panels, and the lowest observed mass loss was 35.5% when coated with boric acid (Îstek et al. 2013). Concrete was mixed with timber joists to manufacture timber-concrete composite floors, which could resist fire longer than 60 min (James et al. 2009). Li et al. (2004) showed that the flame-retarding efficiency of wood plastic polymer composites (WPC) with high-density polyethylene (WPC_{HDPE}) increased to 0.203 and that the limiting oxygen index was 27.1% after the addition of aluminum hydroxide with a weight ratio of 40%. Flame-retardant materials remarkably improved the fire performance of WPC. However, such composites are seldom in engineering structural applications because of their poor dimensional stability, decay resistance, and strength.

Wood-metal composites (WMC) are promising materials because of their high strength and dimensional stability. Most of the research on WMC focuses on characterizing the mechanical properties, electromagnetic shielding, flame retardancy, and decorative values (Schnal et al. 2009; Song and Lam 2012; Lu et al. 2013). The fire performance of WMC with surface coating (White 1983), reinforced joints (Moss et al. 2009), and metal plate connected material (White 1983) was also investigated. Laminated

[a]These authors contributed equally to this work.
[b]We would like to dedicate this paper to Robert H. White, who passed away just before the paper was completed for submission. Robert H. White played an essential role in the research described here, and he is greatly missed.

***Corresponding authors: Keyang Lu,** Research Institute of Wood Industry, Chinese Academy of Forestry, Beijing 100091, People's Republic of China; and USDA Forest Service, Forest Products Laboratory, Madison, WI 53726-2398, USA, e-mail: luky@caf.ac.cn;
Zhiyong Cai: USDA Forest Service, Forest Products Laboratory, Madison, WI 53726-2398, USA, e-mail: zcai@fs.fed.us
Robert H. White and Neil Gribbins: USDA Forest Service, Forest Products Laboratory, Madison, WI 53726-2398, USA
Feng Fu and Yisheng Zhang: Research Institute of Wood Industry, Chinese Academy of Forestry, Beijing 100091, People's Republic of China
Junfeng Hou: Research Institute of Wood Industry, Chinese Academy of Forestry, Beijing 100091, People's Republic of China; and College of Engineering, Zhejiang Agriculture and Forestry University, Lin'an 311300, People's Republic of China

Brought to you by | DigiTop - USDA's Digital Desktop Library
Authenticated
Download Date | 9/25/15 2:38 PM

veneer lumber joints were connected with metal plates, which were covered with graphite phenolic spheres (GPS) (Subyakto et al. 2001), and the results showed that GPS (large or medium-sized sheet) delayed the temperature rise time to 260°C for at least 60 min. The focus of the study of Erchinger et al. (2010) was the fire design of multiple shear steel-to-timber connections with slotted-in steel plates and steel dowels; the material resisted fire for 60 min due to the protection effect of timber boards or gypsum plaster boards. Schaffer (1967a) investigated the flame spread behavior of thin plywood panels with noncombustible inserts placed immediately below the face veneers. The noncombustible inserts included 0.8 mm (1/32 in)-thick 2024-T3 clad aluminum alloy and 0.025 mm (1/1000 in)-thick aluminum foil. Increasing the thickness of the face veneer from 0.4 mm (1/60 in) to 0.9 mm (1/28 in) increased the flame spread index of the panel. The 0.8-mm-thick aluminum sheet insert significantly reduced the flame spread rate, but the aluminum foil did not. The aluminum foil was too thin to resist the pressure of the volatile gases from the wood, and the foil did not always remain intact. As noted in several U.S. patent applications, early fire doors consisted of a wood core faced with metal sheeting.

WMC, as engineered wood products, are widely used in load-bearing structures such as I-joists, studs, large roof spans, and compartment floors. Among metals, aluminum alloy gained high levels of public interest due to its excellent properties of recyclability, formability, light weight, and high strength (Hashim et al. 2005; Fogle et al. 2012). The literature concerning the fire performance of wood-aluminum composites (WAC) is scare. Aluminum alloy foils were overlaid on MDF to prepare WAC, and the results of cone calorimeter testing indicated a decrease of effective heat of combustion of 90.6% and a total heat release of 96.6% (Yang 2012). The fire performance of wood-aluminum laminated composites was not yet tested.

In this study, aluminum alloy sheets were laminated to the oriented strand board (OSB) and the wood veneer to manufacture WAC. Their fire performance was investigated in a small vertical furnace in accordance with ASTM E 119. The mechanical properties of WAC were tested in accordance with ASTM D 1037-06a. The purpose of this study was to provide insights and establish a mathematical model to understand better the fire performance of several types of WAC.

Materials and methods

Aluminum alloy sheets (3003) were obtained from McMaster-Carr Supply Co. (Atlanta, USA). The material has a good weldability, formability, and corrosion resistance, and it is similar to alloy 1100 but has a higher strength due to its manganese content. The size of the aluminum alloy sheet was 900×2400×1.6 mm^3. Isocynate resin (MDI, RUBINATE 1840) was provided by Huntsman Corporation (Salt Lake City, USA); color: dark brown; viscosity at 25°C: 180 cps. This kind of resin is suited for hot pressing. Isoset WD3-C130 resin was provided by Ashland Specialty Chemical Co. (Massachusetts, USA): color: white; viscosity at 25°C; between 2800 and 4500 cps. Isoset CX-47 cross-linking agent was also provided by Ashland; color: black; viscosity at 25°C: between 140 and 260 cps. This kind of resin mixture is suited for cold pressing. The OSB with dimensions of 1200×2400×6.5 mm^3 (Home Depot, Madison, WI, USA) was the basis for the preparation of the composite panels. The resin in the OSB was phenol formaldehyde resin. The wood face veneer was 1.4 mm thick.

Four types of composites were prepared as illustrated in Figure 1A: (a) control panel without any aluminum alloy sheet, (b) composite with 1.6-mm-thick aluminum alloy sheet placed on the surface, (c) composite with 1.6-mm-thick aluminum alloy sheet placed in the middle, and (d) composite with thinner veneer placed on the (b) type of composites. Furthermore, the thickness of the OSB, aluminum alloy sheet, and wood veneer was 6.5, 1.6, and 1.4 mm, respectively. For the hot-pressed composites, the press time was 20 min at 150°C and the pressure was 1 MPa. The cold-pressed composites were prepared at a pressure of 1 MPa for 2 h. The resin usage for the composites was 50 g m^{-2} for each bonding line.

The aluminum alloy sheet has very high surface free energy and has little or no chance of remaining clean for long as it oxidizes easily upon exposure to air, the surface is converted to a lower energy level, and the strength is deteriorated (Arrowsmith and Clifford 1985). Therefore, the sheets were abrasively cleaned by sanding to remove the weak boundary layers of oxide and scale, and this treatment also enhanced their mechanical interlocking with the adhesive.

The specimens were removed from the hot press and stored in plastic bags before fire testing to maintain similar moisture contents (MC) within the test specimens. The normal practice of conditioning at 23°C and 50% relative humidity was not followed for time shortage. Moreover, it was confirmed that the metal facings limit the moisture adsorption of the specimens. Probably, the metal facings resulted in uneven moisture gradients within the specimens and caused inconsistencies in the MC of specimens with and without metal facings. To keep the thermocouples intact, the specimens were not sawed or cut. The specimen size was 510×510 mm^2 (20×20 in.). The specimens tested in the small vertical furnace are listed in Table 1.

The tests were conducted in the Forest Products Laboratory (FPL) small vertical concrete furnace (customer-designed by Forest Products Laboratory, Wisconsin, USA). The specimen sizes were considerably smaller than those required by the ASTM E119 standard. The vertical gas-fired furnace had a square opening (510×510 mm^2; i.e., 20×20 in) for the test specimen (Figure 1B). The furnace had pipe outlets for discharging the natural gas from the furnace. A single-furnace thermocouple was used to control the furnace, which was in a capped metal pipe situated opposite the center of the test specimen in a distance of 50 mm (2 in) from the exposed surface. The flow of natural gas was controlled so that the furnace temperature was also well controllable. Due to the placement of the pipe outlets, the furnace thermocouple was closer to the specimen surface than the 152 mm (6 in) specified in ASTM E119. All air for combustion was admitted by natural draft through side vents near the bottom of the furnace. Most tests were replicated three times. The thermocouples on the unexposed surface were placed underneath the small ceramic fiber pads.

Brought to you by | DigiTop - USDA's Digital Desktop Library
Authenticated
Download Date | 9/25/15 2:38 PM

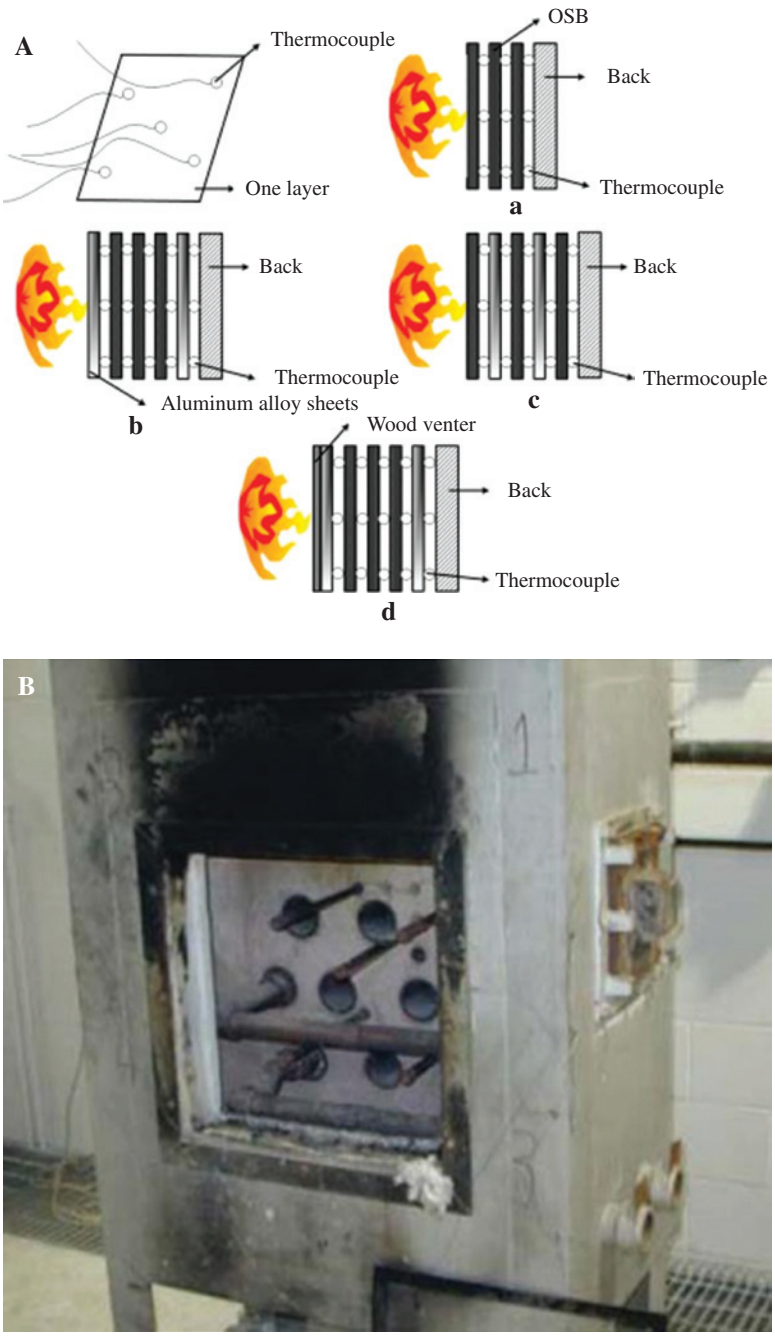

Figure 1 (A) Construction of WAC and position of thermocouples in the composites ("back" was the surface of the composite unexposed to fire during the small vertical furnace test): (a) control panels without any aluminum alloy sheet, (b) 1.6-mm-thick aluminum alloy sheet placed in the middle, (c) 1.6-mm-thick aluminum alloy sheet placed on the surface, and (d) 1.4-mm-thick wood veneer placed on the (c) type of composites. (B) FPL small vertical furnace.

The thermocouples were placed in the overall center of the 510×510 mm^2 panel and in the center of each quadrant. Five thermocouples were placed between each layer (Figure 1A). The thermocouples within or on the specimens were made from 0.25 mm (0.01 in) diameter (30-gauge) chromel/alumel (type K) wires. These thermocouples enabled the recording of the times for temperature increase to an average of 139°C or to T_{max} of 181°C (shortly $T_{139°C/181°C}$). This temperature increase time is one of the failure criteria in ASTM E119 (White 1982).

A series of models were established to analyze the char rate of wooden composites (White 2002; Babrauskas 2005; Tsai et al. 2012). In this study, the baseline of the char layers was determined to be approximately 300°C in accordance with ASTM E119 fire exposure. Therefore, the times for temperature increase to 300°C ($T_{300°C}$) were

Brought to you by | DigiTop - USDA's Digital Desktop Library
Authenticated
Download Date | 9/25/15 2:38 PM

Table 1 Description of the specimens tested in a small vertical furnace.

Composite	Code[a]	No. of tests	Type of pressing	Thickness (mm)
C	O+O+O	3	Cold	18
H	O+O+O	3	Hot	18
CA	A+O+O+O+A	3	Cold	21
HA	A+O+O+O+A	3	Hot	21
HO	O+A+O+A+O	3	Hot	21
HV	V+A+O+O+O+A	3	Hot	23

A, aluminum alloy sheet; C, cold pressing; H, hot pressing; O, OSB; and V, wood veneer.

[a]Code indicates the panel type.

recorded. The char rates were calculated assuming a simple linear model of $T_{300°C}$ divided by the distance from the fire-exposed surface (Table 2) (Schaffer 1967b). The model for the OSB as an outer layer (composites: C, H, and HO) was

$$T_{300°C} = L_{300°C} \times X_C \quad (1)$$

where $T_{300°C}$ is the time to reach 300°C (min), $L_{300°C}$ is the linear char rate parameter (min mm^{-1}), and X_C is the distance (mm) from the fire-exposed surface.

For specimens protected with the aluminum alloy sheet (composites: CA, HA, and HV), a *y*-intercept parameter must be added to Equation (1) to account for the delayed charring of the OSB. The corresponding model is

$$T_{300°C} = L_{300°C} \times X_C + Y_0 \quad (2)$$

where Y_0 was the *y*-intercept parameter (min).

The mechanical properties of WAC were investigated in accordance with ASTM D 1037-06a. The modulus of elasticity (MOE) of WAC was measured by static bending, and the internal bond strength was measured by tension perpendicular to surface (internal bond).

The micrographs of bonding interface between the OSB and the aluminum alloy sheet were investigated by the 3D Analysis System of Super Depth (KEYENCE VHX-1000, Osaka, Japan).

Table 2 Test results of the composites indicated.

Composite	X_C[a] (mm)	Layer no.	Time to reach the *T* (min) 139°C/181°C[b]	300°C[c]	Equation for calculation of $T_{300°C}$ (min)[d]
C	6.2	1	5.0±0.9	8.7±1.2	$1.5X_C$
C	12.4	2	12.3±1.4	19.1±1.1	$1.5X_C$
C	18.6	3	20.6±2.6	23.8±0.4	$1.5X_C$
H	6.2	1	3.7±0.5	7.3±0.5	$1.3X_C$
H	12.4	2	10.8±0.6	16.5±0.6	$1.3X_C$
H	18.6	3	17.8±1.0	22.7±0.8	$1.3X_C$
CA	1.6	1	12.3±3.2	23.2±4.8	$1.6X_C+21.0$
CA	7.6	2	22.7±1.5	32.7±5.2	$1.6X_C+21.0$
CA	13.6	3	33.5±6.3	44.0±4.5	$1.6X_C+21.0$
CA	19.6	4	42.9±4.9	51.2±4.4	$1.6X_C+21.0$
CA	21.2	5	44.8±4.6	55.4±6.1	$1.6X_C+21.0$
HA	1.6	1	9.9±1.4	23.9±1.7	$1.3X_C+21.6$
HA	7.6	2	19.2±1.4	32.0±1.7	$1.3X_C+21.6$
HA	13.6	3	31.8±2.4	40.3±1.6	$1.3X_C+21.6$
HA	19.6	4	39.1±2.6	45.9±2.3	$1.3X_C+21.6$
HA	21.2	5	41.6±3.0	48.9±3.1	$1.3X_C+21.6$
HO	6.0	1	4.9±0.1	9.7±0.4	$1.6X_C$
HO	7.6	2	7.3±0.4	14.2±0.4	$1.6X_C$
HO	13.6	3	15.2±0.5	20.6±0.4	$1.6X_C$
HO	15.2	4	17.8±0.1	24.0±0.2	$1.6X_C$
HO	21.2	5	23.6±1.0	25.7±0.1	$1.6X_C$
HV	3.0	1	2.4±0.9	9.8±0.4	$1.7X_C+5.9$
HV	9.0	2	10.4±0.2	23.2±2.5	$1.7X_C+5.9$
HV	15.0	3	20.4±0.5	33.1±3.0	$1.7X_C+5.9$
HV	21.0	4	34.3±3.4	41.3±3.6	$1.7X_C+5.9$
HV	22.6	5	35.6±2.8	43.9±2.8	$1.7X_C+5.9$

For abbreviations, see Table 1.

[a]X_C distance from the fire-exposed surface.

[b]Time (*T*, mean±SD of three replicates) for the unexposed surface of each layer of WAC to reach an average $T_{139°C}$ or $T_{max,181°C}$ above room temperature.

[c]Time (*T*, mean±SD of three replicates) for the unexposed surface of each layer of WAC to reach an average $T_{300°C}$. In some cases, some individual thermocouples of the last layer (i.e., layer 3 or 5) did not record a $T_{300°C}$ or were influenced by ignition and flame spread over the unexposed surface at the end of the test. This is the reason why sometimes the values for the last layer are less than expected.

[d]Linear char rate equations to reach 300°C. Data obtained from the thermocouples of the unexposed surface were not considered to obtain Equation (1) or (2). See footnote b for rationale.

Results and discussion

Numerical results

Table 2 shows the test results for $T_{139°C/181°C}$, $T_{300°C}$, and the linear char rate models (*L*) of the different composites. The total $T_{139°C/181°C}$ of all composites ranged from 17.8 to 44.8 min. Individually, the lamination of the aluminum alloy sheet (except in the middle) significantly improved the fire performance. For hot-pressed composites, the following $T_{139°C/181°C}$ order was found: HA>HV>HO>H. Composite CA had the longest $T_{139°C/181°C}$ among all composites. The results were similar for the total $T_{300°C}$. These results are illustrated in Figure 2a.

The char rates for the two models [Equations (1) and (2)] were calculated from the corresponding times and distances from the exposed surface (Table 2). The $L_{300°C}$ for the OSB specimens without any aluminum alloy sheet (C and H) was 1.5 and 1.3 min mm^{-1}, respectively. The $L_{300°C}$ for the corresponding OSB with the aluminum alloy sheet (CA and HA) was slightly higher (1.6 and 1.3 min mm^{-1}). These values indicated a slightly faster charring than the linear

Brought to you by | DigiTop - USDA's Digital Desktop Library
Authenticated
Download Date | 9/25/15 2:38 PM

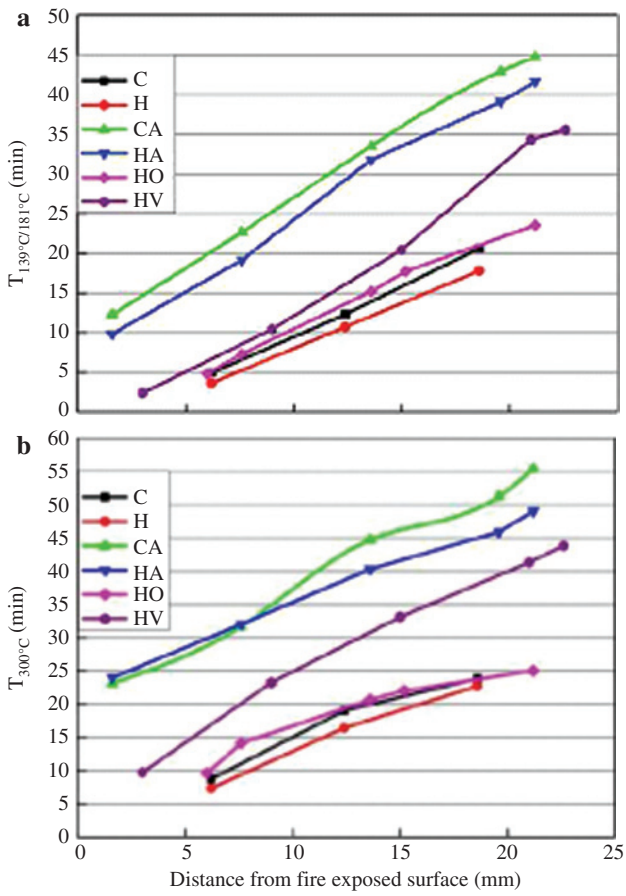

Figure 2 Plots of the times for 139°C/181°C (a) and 300°C (b) increase in temperature at various distances from the fire-exposed surface.

charring rate of 1.6 min mm^{-1} (0.6 mm min^{-1}, 38 mm h^{-1}, and 1.5 in h^{-1}) generally assumed for the charring of a semi-infinite slab of solid wood or glued laminated lumber. The results were consistent with the results of 1.42–1.47 min mm^{-1} reported for 28- to 30-mm-thick OSB rim boards (White 2003). For the specimens without any aluminum alloy sheet, the regressions with a nonzero *y*-intercept [Equation (2)] confirmed that the *y*-intercept is small and that the zero-intercept model [Equation (1)] was appropriate. The specimens with the aluminum alloy sheet on the surface confirmed the need for a nonzero intercept in the model [Equation (2)] (Table 2) due to an initial delay in the charring. These conclusions were consistent with the results illustrated in Figure 2a and b.

Visual observation

The main observations of fire test specimens are shown in Figure 3. For composite H, the surface layer of the OSB ignited and burned down in 10 min (Figure 3a). The second layer of the OSB also combusted and turned gray in 15 min. After a continuous exposure to fire, charred holes appeared on the backside of the panel and the entire panel burned away in 25 min (Figure 3b). In the case of composite HA, some resin came out with the smoke after 15–20 min when the aluminum alloy sheet was located on the surface (Figure 3c). The first layer of the aluminum alloy sheet melted in 25 min. The OSB burned out in 55 min and the second aluminum alloy sheet was delaminated from the OSB and completely melted in 60 min (Figure 3d). Composite HO started to burn and turned black after 10 min of exposure. Large amounts of smoke were released during the combustion of the OSB (Figure 3e). The first layer of the aluminum alloy sheet was separated from the OSB and melted in 20 min followed by the combustion of the OSB, and the second layer of the aluminum alloy sheet fell off the specimen in 30 min. For composite HV, the wood veneer combusted quickly in 5 min (Figure 3f). The first layer of the aluminum alloy sheet started to melt in 25 min. The OSB burned up and the second layer of the aluminum alloy sheet melted in 50 min.

Regression model of the times to reach $T_{300°C}$

The linear regression data were calculated based on the complete data set for the times to reach 300°C ($T_{300°C}$) as a function of the composite construction. The unexposed surface of WAC was excluded from the data set. The resulting equation for $T_{300°C}$ at a distance X_C from the fire-exposed surface was

$$T_{300°C} = 1.31X_C + 0.24M * X_C + 19.27M + 1.94P + 2.17\,\mathrm{HO} - 11.02\mathrm{HV} \quad (3)$$

where M=1 for the specimens with the aluminum alloy sheet on the exposed surface with or without the wood veneer covering (CA, HA, and HV) and M=0 for the ones with exposed OSB (C, H, and HO). P=1 for the OSB made by cold pressing (C and CA) and P=0 for the OSB made with hot pressing (H, HA, HO, and HV).

HO=1 for the specimen type HO with the aluminum alloy sheet in the interior and HO=0 for the rest. HV=1 for the specimen type HV with the wood veneer covering the aluminum sheet and HV=0 for the rest. The more significant parameters in the equation were HV, M, and X_C with P_r>t of <0.0001. The less significant parameters of P, HO, and M*X_C had P_r>t data (i.e., 0.047, 0.112, and 0.049) being >0.0001. The equation accounted for most of the variations with an R^2 of 0.99. With regard to the statistics,

Brought to you by | DigiTop - USDA's Digital Desktop Library
Authenticated
Download Date | 9/25/15 2:38 PM

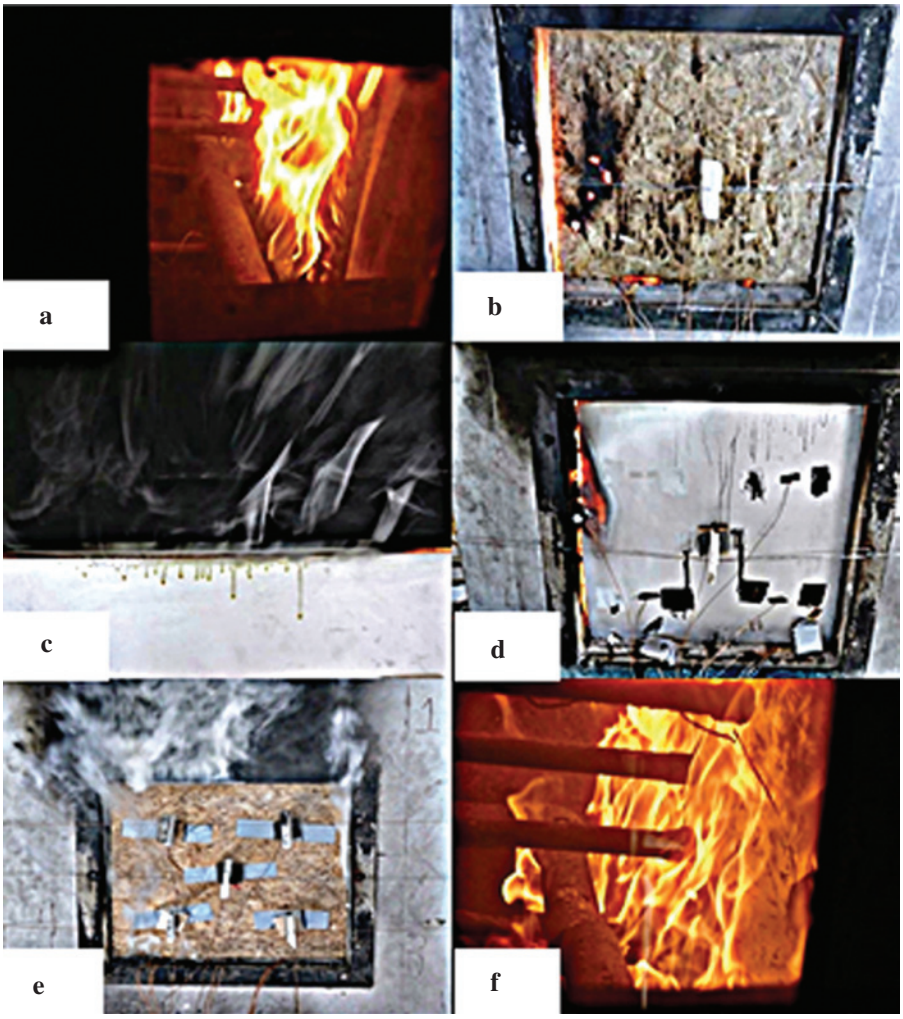

Figure 3 Photos and approximate observation time (the approximate observation time was in the curve behind the specimen name) of WAC during the small vertical furnace test: (a) composite H (5 min), (b) composite H (24 min), (c) composite HA (20 min), (d) composite HA (50 min), (e) composite HO (15 min), and (f) composite HV (5 min).

it should be noted that the 60 observations in the analysis were not completely independent, as multiple readings came from each of the 18 tests included in the analysis.

Comparison of the press method

The comparison of the composites under different press methods is listed in Tables 2 and 3(a) and Figures 2a and 4a and b. As observed from the results in Table 2, the $L_{300°C}$ was 1.5 min mm^{-1} for composite C with a density of 738 kg m^{-3}, 1.30 min mm^{-1} for composite H with a density of 730 kg m^{-3}, 1.6 min mm^{-1} for composite CA with a density of 1072 kg m^{-3}, and 1.3 min mm^{-1} for composite HA with a density of 969 kg m^{-3}. It is visible that the cold-pressed OSB with higher density has a lower $L_{300°C}$ (Figure 4a and b). The overall linear regression model [Equation (3)] indicates those times for $T_{300°C}$ 1.9 min longer with the cold-pressed OSB.

Table 3(a) and Figure 2a show the $T_{139°C/181°C}$ improvement in each layer of the composite. The $T_{139°C/181°C}$ difference concerning the composite without the lamination of the aluminum alloy sheet ranged from 1.3 to 2.8 min (average of 1.9 min). That of WAC ranged from 1.7 to 3.8 min (average of 2.9 min). The thermal resistance along the thickness plane increased due to increased density and contributed to the observed subtle L differences. The larger is the thermal resistance, the greater is $L_{300°C}$. The presented data here support those of White (2002) and Schaffer (1967b) concerning the $L_{300°C}$ increment as a function of density.

Brought to you by | DigiTop - USDA's Digital Desktop Library
Authenticated
Download Date | 9/25/15 2:38 PM

Table 3 $T_{139°C/181°C}$ difference (min) of each layer (*L*) of the composites: (a) composites under different press methods (H and HA for hot pressing and C and CA for cold pressing), (b) lamination with or without any aluminum alloy sheet (C and H without any aluminum alloy sheet, CA and HA with the aluminum alloy sheet on the surface, and HO with the aluminum alloy sheet in the middle), and (c) lamination with or without the wood veneer (HA without the wood veneer and HV with the wood veneer on the surface of the aluminum alloy sheet).

	$T_{139°C/181°C}$ difference (min) for the layers				
Composites	***L*1**	***L*2**	***L*3**	***L*4**	***L*5**
(a)					
H vs. C	1.3	1.6	2.8		
HA vs. CA	2.4	3.6	1.7	3.8	3.2
(b)					
C vs. CA		17.8	21.2	22.3	
H vs. HA		15.5	21.0	21.3	
HO vs. HA		11.9	16.6		18.1
HO vs. H	1.2		4.4		5.8
(c)					
HV vs. HA	7.5	8.7	11.4	4.8	6.0

Effect of the aluminum alloy sheet

The influence of the aluminum alloy sheet on the fire performance of WAC is shown in Table 3(a) and Figures 2a and 4c–f. The results in Table 3(a) indicate that the $T_{139°C/181°C}$ improvement of each layer for cold0pressed specimens was 17.8, 21.2, and 22.3 min with an average of 20.4 min. The corresponding data of hot-pressed specimens are 15.5, 21.0, and 21.3 min with an average of 19.3 min (see also Figure 2a). The composites with the aluminum alloy sheet on the laminate surface needed a remarkably longer total time for destruction than the composites without any aluminum alloy sheet. The overall regression model [Equation (3)] shows an average delay in the charring of the OSB ($T_{300°C}$) of 19.3 min with the aluminum alloy sheet on the laminate surface.

The aluminum alloy sheet with a thickness of 0.1 mm adhered to the surface of carbon fiber-reinforced composites by Chang and Zheng (2005) to improve their thermal resistance because of its excellent thermal conductivity. The temperature differences of the various areas diminished with time, and the thermal resistance along with the thickness significantly increased with the aluminum alloy sheet on the surface (Figure 4c and d). This prevents a rapid temperature increase along with the thickness. The heat dissipation potential of the aluminum alloy sheet should be emphasized; that is, the aluminum alloy sheet on the surface is a kind of heat radiator and reflector and prevents the rapid heating of the OSB (Subyakto et al. 2001). Moysey and Muir (1968) worked with shiny galvanized steel or aluminum on wood and estimated that the time for ignition of wood was four times longer with these materials on the surface. With the metal cladding painted or smeared with mud, the effect was essentially deteriorated because of hindering the ionizing radiation.

The $T_{139°C/181°C}$ difference for the composites with the aluminum alloy sheet in different positions (HO vs. HA) was 11.9, 16.6, and 18.1 min [Table 3(b)]. The temperature for composite HO rose faster than that of composite HA (Figure 4e). Expectably, HO initially behaved more like composite H than composite HA [Table 3(b); Figures 2a and 4f]. For composite HO, the combustion performance of the first layer of the OSB was a critical point. The heat reflection ability of the aluminum alloy sheet diminished with the OSB on the surface. Therefore, the influence of the aluminum alloy sheet on the first layer of the OSB was very small. After burning the OSB layer, the interior aluminum alloy sheet became a surface aluminum alloy sheet. As a result, there was a small increase in $T_{139°C/181°C}$ over that for composite H [Table 3(b); Figure 2a]. In summary, laminates with the aluminum alloy sheet in the middle provided minimal improvement in the fire performance of WAC. In the overall regression charring model [Equation (3)], the addition of the aluminum alloy sheet in the interior increased the $T_{300°C}$ by 3.1 min.

Effect of the wood veneer

The effect of the wood veneer on the fire performance of WAC is presented in Table 3(c) and Figures 2a and 4g). The $T_{139°C/181°C}$ of each layer was reduced by 7.5, 8.7, 11.4, 4.8, and 6.0 min, respectively, after the lamination of the wood veneer on the surface of the aluminum alloy sheet (HV shown in Figure 1A and Table 1) as shown in Table 3(c). The average reduction time was 7.7 min. The results indicated that the fire performance of WAC decreased if the wood veneer was on the surface (Figure 4g). In the overall regression charring model for $T_{300°C}$ [Equation (3)], the addition of the wood veneer to the aluminum alloy sheet reduced the $T_{300°C}$ by 11 min. This is in contrast to the improvement of 19.3 min provided with the aluminum alloy sheet on the surface of the OSB. As illustrated in Figure 4g for $T_{139°C/181°C}$, the composite with the wood veneer (HV) on the aluminum alloy sheet initially behaved like the exposed OSB (H), but later on the $T_{139°C/181°C}$ was more consistent in the case of composite HA. This can be explained by the heat reflection of the aluminum alloy sheet after the wood veneer was burned off.

Modulus of elasticity

The static MOE of different composites is shown in Table 4. The MOE value of composite HA, which was parallel or

Brought to you by | DigiTop - USDA's Digital Desktop Library
Authenticated
Download Date | 9/25/15 2:38 PM

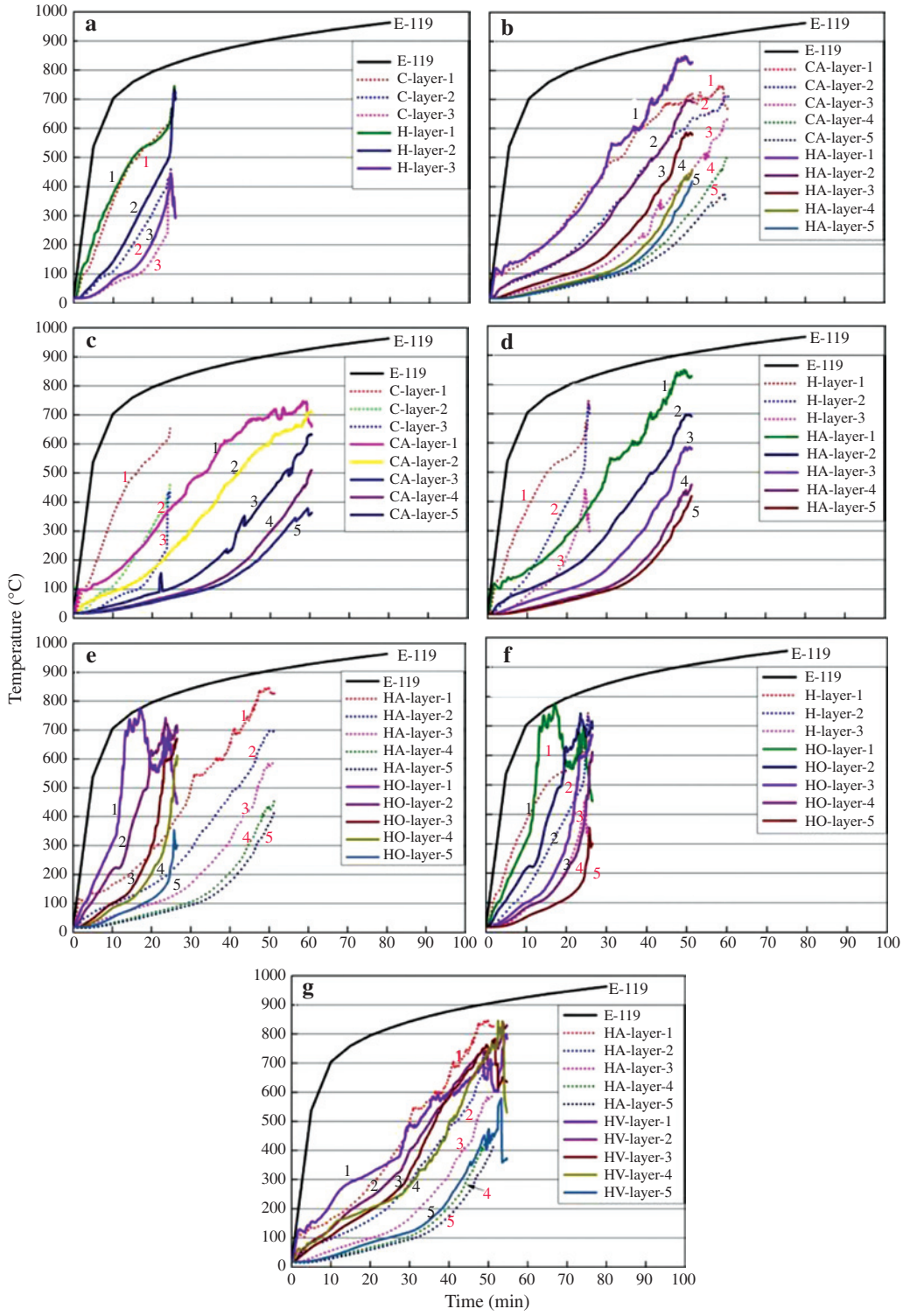

Figure 4 Time-temperature curve of different composites: (a) composite C vs. composite H, (b) composite CA vs. composite HA, (c) composite C vs. composite CA, (d) composite H vs. composite HA, (e) composite HA vs. composite HO, (f) composite H vs. composite HO, and (g) composite HA vs. composite HV.

perpendicular to the OSB, increased by 309% (14.091 GPa) and 485% (14.57 GPa), respectively. Meantime, the MOE of composite HO exceeded that of composite H by about 62% (3.431 GPa), which was parallel to the OSB, and that of the perpendicular to the OSB was about 166% (4.36 GPa). Obviously, the lamination of the aluminum alloy sheet

Brought to you by | DigiTop - USDA's Digital Desktop Library
Authenticated
Download Date | 9/25/15 2:38 PM

Table 4 MOE of different specimens parallel (||) and perpendicular (⊥) to OSB orientation

	MOE (||) to the OSB		MOE (⊥) to the OSB	
Composite	Mean[a]±SD (GPa)	CV[a] (%)	Mean±SD (GPa)	CV (%)
O[b]	3.6±0.9	25.0	1.7±0.4	24.6
H	4.6±0.3	7.6	3.0±0.1	2.2
HA	18.6±0.9	4.7	17.6±0.9	5.1
HO	8.0±0.1	1.0	7.4±0.3	4.0

[a]Mean is for repeated specimens. CV is coefficient of variation.
[b]Composite O has a single layer of the OSB.

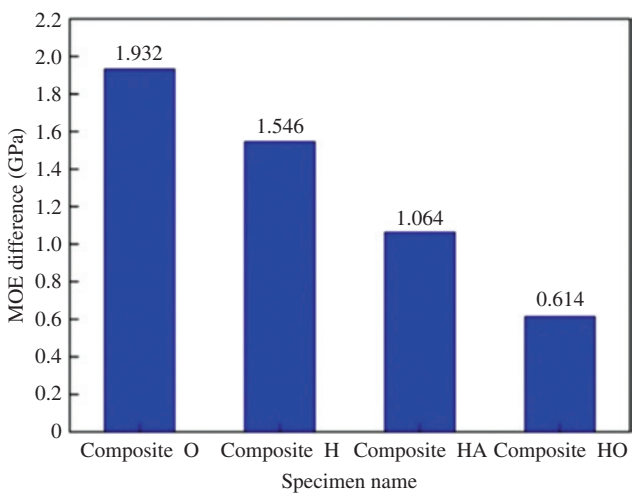

Figure 5 MOE (for the OSB and WAC) difference between parallel and perpendicular to the OSB (composite O was the composite with a single layer of the OSB).

in the middle (HO) or on the surface (HA) significantly enhanced the composite strength (HO and HA shown in Figure 1A and Table 1). It was also noted that the incremental strength of composite HA was significantly greater than that of composite HO. The reason was that the MOE increased with the increasing distance between the aluminum alloy sheet and the core layer (Arani et al. 2011). As a consequence, composite HA exhibited the largest MOE among the entire composites.

Figure 5 shows the MOE difference between parallel and perpendicular to the OSB. The difference of MOE between parallel and perpendicular to the OSB decreased due to the isotropic and excellent mechanical performance of the aluminum alloy sheet laminated with the OSB. The uniformity and strength of the composites was enhanced due to the lamination of the aluminum alloy sheet.

Internal bond strength

Figures 6 and 7 show the bonding interface between the aluminum alloy sheet and the OSB. It was found that the MDI dispersed sufficiently and formed excellent mechanical interlocking between the OSB and the aluminum alloy sheet. A compact and continuous glue layer was efficiently generated. Rupture was observed to occur in the core of the OSB for the entire composites (Figure 7). It was concluded that the bonding strength between the OSB and the aluminum alloy sheet was greater than the internal bond strength of the OSB.

Conclusion

The fire performance of WAC was investigated in accordance with ASTM E119. The $T_{139°C/181°C}$ of different composites ranged from 17.8 to 44.8 min. It was also indicated that the position of the aluminum alloy sheet significantly affected the fire performance of WAC. The $T_{139°C/181°C}$ was improved and more than doubled after the lamination of the OSB with

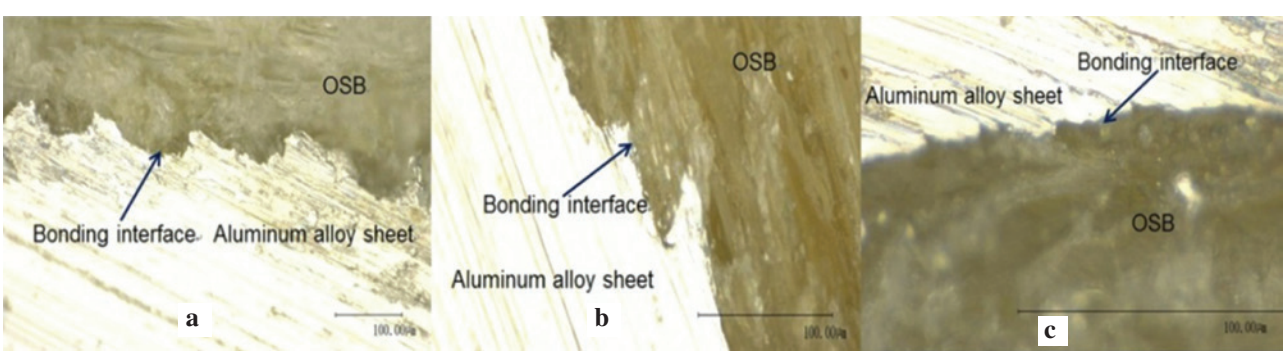

Figure 6 Bonding interface between the aluminum alloy sheet and the OSB. Magnification, ×500, ×1000, and ×2000 (a–c, respectively).

Brought to you by | DigiTop - USDA's Digital Desktop Library
Authenticated
Download Date | 9/25/15 2:38 PM

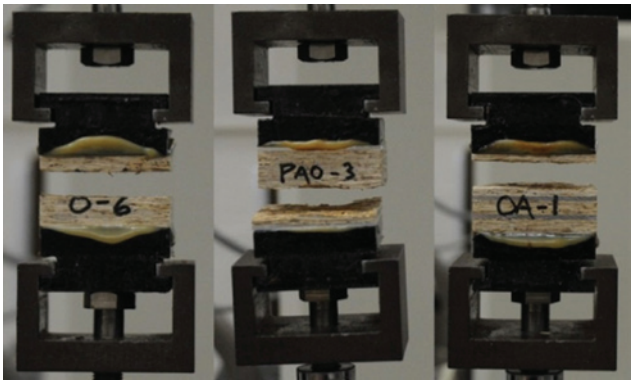

Figure 7 Reference photo for tension testing perpendicular to the surface (internal bond) of the specimen.
The specimen size was 51×51 mm^2 (2×2 in).

the aluminum alloy sheet. The cold-pressed composites showed better fire performance than the hot-pressed composites. The fire performance of composite with 1.6-mm-thick aluminum alloy sheet located on the surface was best followed by the composite with 1.4-mm-thick wood veneer on the surface of the aluminum alloy sheet and then by the composite without any aluminum alloy sheet for the hot-pressed composites. The lamination of the wood veneer on WAC surface detracted the fire performance. The positioning of the aluminum alloy sheet in the middle of the composite provided little improvement in the fire performance compared with the OSB without any aluminum alloy sheet. The MOE values quadrupled when the aluminum alloy sheet was located on the surface. The bonding strength between the OSB and the aluminum alloy sheet was greater than the internal bond strength of the OSB alone.

Acknowledgments: The authors thank the industry special fund project (201104004) and outstanding scholar teaching plan of Chinese Academy of Forestry (CAF) for supporting this paper. We also greatly appreciated associate Professor Youming Yu (Zhejiang Agriculture & Forestry University) for his technical assistance during the analyzing of bonding interface.

References

Arani, A.G., Maghamikia, S., Mohammadimehr, M., Arefmanesh, A. (2011) Buckling analysis of laminated composite rectangular plates reinforced by SWCNTs using analytical and finite element methods. J. Mech. Sci. Techn. 25:809–820.

Arrowsmith, D.J., Clifford, A.W. (1985) A new pretreatment for the adhesive bonding of aluminum. Int. J. Adhes. Adhes. 5:40–42.

Babrauskas, V. (2005) Charring rate of wood as a tool for fire investigations. Fire Safety J. 40:528–554.

Chang, X.Q., Zheng, G.T. (2005) Three-dimensional heat transfer analysis to hybrid multilayer composite structure. Chin. J. Appl. Mech. 22:633–637.

Erchinger, C., Frangi, A., Fontana, M. (2010) Fire design of steel-to-timber dowelled connections. Eng. Struct. 32:580–589.

Fogle, E.J., Lattimer, B.Y., Feih, S., Kandare, E., Mouritz, A.P., Case, S.W. (2012) Compression load failure of aluminum plates due to fire. Eng. Struct. 34:155–162.

Hashim, R., How., L.S., Kumar, R.N., Sulaiman, O. (2005) Some of the properties of flame retardant medium density fiberboard made from rubber wood and recycled containers containing aluminum trihydroxide. Bioresource Technol. 96:1826–1831.

Îstek, A., Aydemîr, D., Eroğlu, H. (2013) Combustion properties of medium-density fiberboards coated by a mixture of calcite and various fires retardant. Turk J. Agric. For. 37: 642–648.

James, O., David, C., Peter, J.M., Massimo, F., Andrew, H.B. (2009) Fire performance of timber-concrete composite floors. NZL Tim. Des. J. 19:4–13.

Li, B., Jiang, H.L., Zhang, S.F., Wang, Y.F., Sui, X.Y. (2004) Influence of aluminum hydroxide on flame retardancy and mechanical properties of PE-HD/wood flour composites. J. Chin. Plast. 6:21–23.

Lu, K.Y., Fu, F., Sun, H.L., Fu, Y.J. (2013) Bonding technology of electromagnetic shielding plywood laminated with conductive sheets. Wood Res. Slov. 58:465–474.

Moss, P.J., Buchana, A.H., Fragiacomo, M., Lau, P.H., Chuo, T. (2009) Fire performance of bolted connections in laminated veneer lumber. Fire Mater. 33:223–243.

Moysey, E.B., Muir, W.E. (1968) Pilot ignition of building materials by radiation. Fire Technol. 4:46–50.

Schaffer, E.L. (1967a) Charring Rate of Selected Woods – Transverse to Grain. Forest Products Laboratory. USDA Forest Service, Forest Products Laboratory, Madison, WI. pp. 1–28.

Schaffer, E.L. Effect of Panel Thickness and Noncombustible Inserts on Surface Flammability of Plywood. Research Note FPL-152. USDA Forest Service, Forest Products Laboratory, Madison, WI, 1967b.

Schnal, S., Planinc, I., Turk, G. (2009) Fire analysis of timber composite beams with interlayer slip. Fire Safety J. 44:770–778.

Song, X.B., Lam, F. (2012) Stability analysis of metal-plate-connected wood truss assemblies. J. Struct. Eng. 138:1110–1119.

Subyakto, B., Hata, T., Ide, I., Kawai, S. (2001) Fire-resistant performance of a laminated veneer lumber joint with metal plate connectors protected with graphite phenolic sphere sheeting. J. Wood Sci. 47:199–207.

Tsai, K., Carradine, D., Moss, P., Buchanan, A. (2012) Charring rates for double beams made from laminated veneer lumber. Fire Mater. 37:58–74.

Urso, V.M., Gibson, A.G. (2009) Fire model for fiber reinforced plastic composites using apparent thermal diffusivity (ATD). Plast. Rubber Compos. 38:87–92.

White, R.H. (1982) Wood-Based Paneling as Thermal Barriers. USDA Forest Service, Forest Products Laboratory, Madison, WI. pp. 1–12.

White, R.H. (1983) Use of coating to improve fire resistance of wood. In: The Need for Standards. ASTM STP 826. Eds. Morris, L., Stumpf, F.M. ASTM. pp. 24–39.

Brought to you by | DigiTop - USDA's Digital Desktop Library
Authenticated
Download Date | 9/25/15 2:38 PM

White, R.H. (2002) Analytical methods for determining fire resistance of timber members. In: The SFPE Handbook of Fire Protection Engineering. Section 4, Chapter 11, 3rd ed. NFPA, Quincy, MA. Vol. 4. pp. 257–273.

White, R.H. (2003) Fire Resistance of Engineered Wood Rim Board Products. Forest Products Laboratory. pp. 1–22.

White, R.H., Cramer, S.M., Shrestha, D.K. Fire Endurance Model for a Metal-Plate-Connected Wood Truss. FPL-RP-522. USDA Forest Service, Forest Products Laboratory, Madison, WI, 1993.

Winandy, J.E., Wang, Q.W., White, R.H. (2008) Fire-retardant-treated strandboard: properties and fire performance. Wood Fiber Sci. 40:62–71.

Yang, H.Q. (2012) Preparation and properties of aluminum/wood decorative composite. Chin. Acad. For. 56–68.

Zhang, Z.X., Zhang, J., Lu, B.X., Xin, Z.X., Kang, C.K., Kim, J.K. (2012) Effect of flame retardants on mechanical properties, flammability and foamability of PP/wood-fiber composites. Compos. Part B Eng. 43:150–158.

Brought to you by | DigiTop - USDA's Digital Desktop Library
Authenticated
Download Date | 9/25/15 2:38 PM